Scientific Research Publishing

Journal of Modern Physics, 2022, 13, 768-775
https://www.scirp.org/journal/jmp
ISSN Online: 2153-120X
ISSN Print: 2153-1196

Anderson Localization Light Guiding in a Two-Phase Glass

Nicholas F. Borrelli, Thomas P. Seward, Karl W. Koch, Lisa A. Lamberson

Corning Inc. Sullivan Park Research Laboratory, New York, USA
Email: Borrellinf@Corning.com, Sewardtp@gmail.com, Kochkw@Corning.com, Lambersola@corning.com

How to cite this paper: Borrelli, N.F., Seward, T.P., Koch, K.W. and Lamberson, L.A. (2022) Anderson Localization Light Guiding in a Two-Phase Glass. *Journal of Modern Physics*, **13**, 768-775.
https://doi.org/10.4236/jmp.2022.135045

Received: February 25, 2022
Accepted: May 28, 2022
Published: May 31, 2022

Abstract

Anderson localization has been realized in several different systems over the years. In this paper we describe a rather unique manifestation of the phenomenon occurring in a two-phase glass composition that guides light. The glasses are a borate or alkali borosilicate composition that when heated separates into two distinct phases of different compositions, a high index phase and a low index phase. When the glass is heated with a specific thermal schedule to develop the phase separation it is then drawn into a rod or fiber, the particulate phase forms elongated strands resulting in a random cross-sectional refractive index pattern. This pattern of refractive index is maintained along the length producing a light guiding behavior over a significant distance that we propose is a manifestation of an Anderson localization phenomenon.

Keywords

Anderson Localization, Imagining Optical Fiber, Phase Separated Glass

1. Introduction

The following paper is an attempt to connect what, at first glance, appears to be an unrelated phenomenon in glass to an example of Anderson localization using the common themes involving waves and disorder. This common behavior of localization in all cases results from wave interference. The unique insight of Anderson [1] was utilizing the Schrodinger equation to treat the diffusion of defects in crystals. What was the natural approach for treating the behavior of photons and phonons was now used for electrons to explain how localized states could occur as a consequence of structural disorder. The physical description of disorder is different for electrons with dopants in an otherwise perfect lattice than for photons where the disorder would correspond to fluctuations of the refractive index; for acoustic phonons it would be regions of different velocities of

sound. (Equation (3)) Clearly, the specific wave equations governing the different wave phenomena are not the same as well as the resulting incorporation of the disorder. For these two examples the disorder is incorporated from the refractive index and the sound velocity, respectively. For the electron case the Hamiltonian is altered either by letting the defect have a broad distribution of energies or letting the potential function $V(r)$ vary spatially. As we will see in the case of electrons for the Anderson treatment to be operative requires that there is ignorable interaction between sites so that the wavefunction of the defect can be uniquely defined. For photons and phonons this is always the case. A simple statement can be made; Waves + Disorder = Localization.

Localized states for photons become localized propagating modes. It appears that one could have arrived at this directly from Maxwell's equations because interference phenomena is inherent in light propagation in a medium with a spatially varying refractive index as we will see below, but here we interpret as an example of Anderson localization.

$$\nabla\times\nabla\times E+\frac{\varepsilon}{c^2}\frac{\partial^2 E}{\partial t^2}=\frac{4\pi}{c^2}\frac{\partial^2 P^{NL}}{\partial t^2} \tag{1}$$

For the 2-D case one can write the nonlinear wave equation (Equation (1)) with an intensity dependent refractive index but now one replaces this term with a static spatial refractive index variation shown here in Equation (2).

$$\frac{i\partial E}{\partial z}=\left(\frac{1}{2k}\right)\nabla_T^2 E+\left(\frac{\int_2}{n_0^2}\right)k\left|E^2\right|E=0 \tag{2}$$

$$\frac{i\partial A}{\partial z}+\left(\frac{1}{2k}\right)\nabla_T^2 A+\left(\frac{k}{n_0}\right)\Delta n(x,y)A=0 \tag{3}$$

Equation (3) appears similar to the Schrodinger equation [2] [3] shown below in Equation (4); where the disorder is represented in the potential wells, $V(r)$ of the electrons on the various sites.

$$ih\frac{\partial\varphi}{\partial t}+\left(\frac{ih^2}{2m}\right)\nabla^2\varphi+\Delta V(r)\varphi(r,t)=0 \tag{4}$$

From the similarity one can work it backward; viz. localized optical modes from disorder by analogy implies localized electronic states as "a wave is a wave".

2. Optical Material Examples

1) Mixed polymers

Below is shown an example of redrawing a mix of two polymer optical fibers of differing refractive index [4]. This can be interpreted as propagating modes via the Anderson localization phenomenon as long the light is not confined to the higher index fiber. The first picture in **Figure 1** shows an SEM image resulting from the co-drawing of the 50 - 50 mix of two 0.25-mm polymer fibers with different refractive indices, thus resulting in a refractive index pattern through which light guiding occurs from the Anderson localization phenomenon.

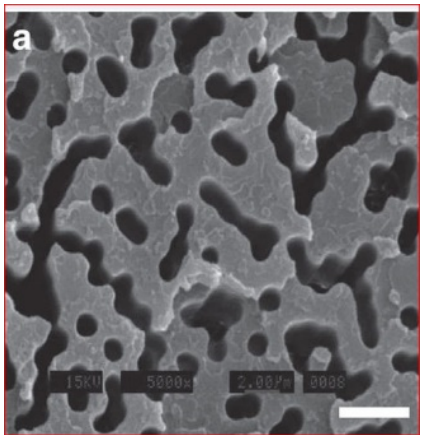

Figure 1. Polymer fiber constructed from 40k PMMA filaments and 40k PS filaments; SEM of the fused and drawn mixture, where one composition has been differentially etched to provide surface relief between the two compositions to enhance the visibility of the compositional structure [4].

2) Glass

The next example of a fiber made from the elongation of phase separated glass [5] [6]. This glass undergoes a liquid-liquid phase separation on heating, (see **Figure 2**). The elongation of the droplets seen in **Figure 2** is produced in the present case by what is termed a down-draw method. Here, by gravity, the glass flows out of a hole in the bottom of the crucible at the appropriate viscosity (temperature) and is formed into a fiber. The observation of image transport in these fibers is indicative of Anderson localization. Light launched into an arbitrary point at the input face of the fiber, emerges in the same transverse location on the output face. The processing method used to create these fibers is more adaptable to a manufacturing process than one based on stacking filaments of different compositions.

The elongated regions are continuous thoughout the length of the fiber as shown in **Figure 2(a)** and a cross sectional view in shown in **Figure 2(b)** showing the random refractive index pattern.

One can obtain an estimate of the relationship between the initial phase droplet size and the ultimate length of the continuous fiber that can result. We utilize the volume conservation of the particles in the blank with radius, R as it relates to the filament radius, r over a length, L. Then, by conservation of volume, we have the following.

$$\frac{4}{3}\pi R^3 = \pi r^2 L\,. \tag{5}$$

Solving for the initial particulate radius we have

$$R = \left(\frac{3r^2 L}{4}\right)^{1/3} \cong 0.909\left(r^2 L\right)^{1/3} \tag{6}$$

One can see from **Figure 3** that for a 10-μm droplet that the fiber radius would be ~0.1 μm for the fiber length of 30 cm and ~0.5 μm for a 2-cm length.

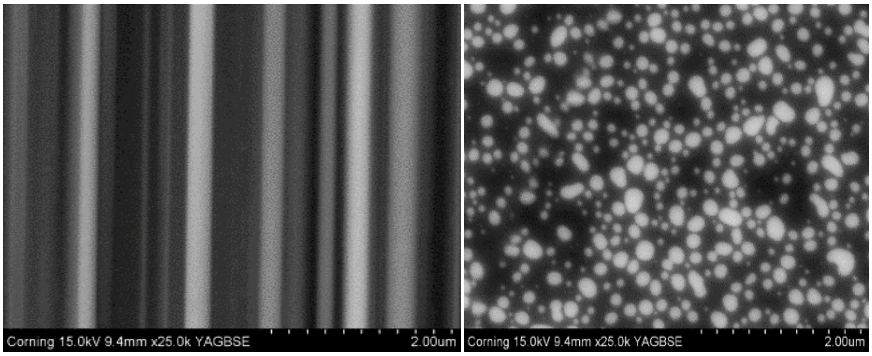

(a)

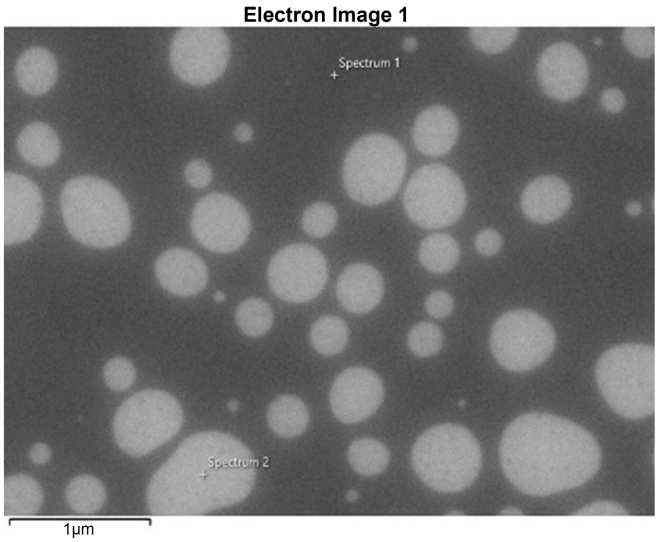

(b)

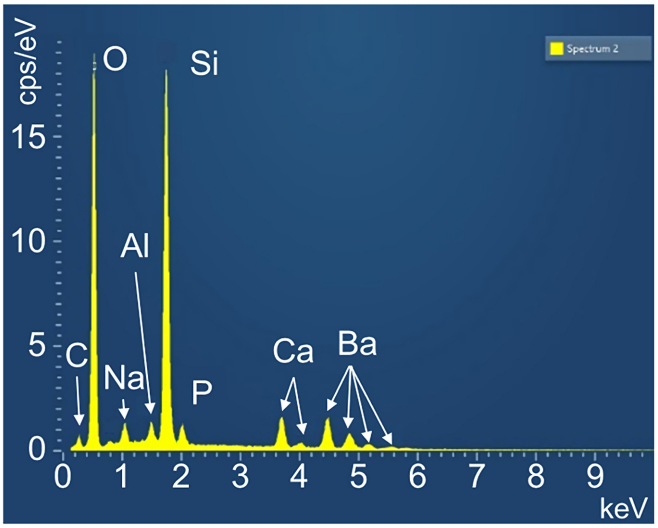

(c)

Figure 2. (a) SEM of a borosilicate composition fiber viewed parallel to the fiber axis (left) and viewed in cross section (right); white regions are the higher index particulate (discontinuous) phase. (b) SEM of the fiber shown in (a), but at higher magnification to show the areas from which chemical element identifications were made. (c) Compositional analysis of the particulate (discontinuous) phase obtained from the SEM images.

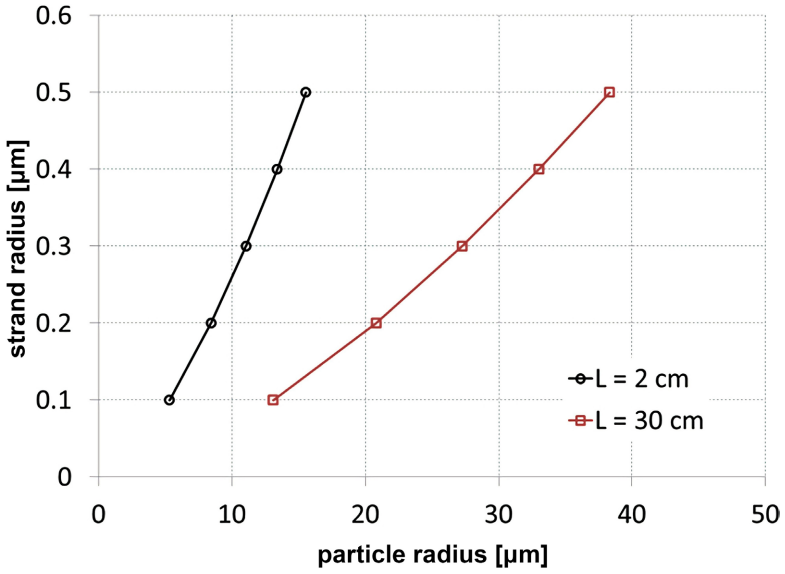

Figure 3. Computed fiber radius as a function of the droplet radius for two different redrawn lengths.

3. Light Guiding Mechanism

It is useful at this point to be more specific about the proposed light guiding mechanism. The light is not guided by the elongated particles (strands) per se, this would not represent Anderson localization. The light guiding is by regions of the index pattern where *regions* of high index are surrounded by *regions* low index. The actual delta *n* is not that of the refractive of respective phases, rather by the difference of the effective indices of the two respective regions. Therefore, this results in a distribution of the values of delta *n* and effective light guiding radii. This is consistent with why we see the guiding behavior irrespective of whether the droplets are the high (borosilicate glass case) or low index phase (borate glass). So truly the light propagation is determined by Equation (2), namely Anderson localization.

4. Mode Calculation

In this section a calculation of the possible propagating modes is accomplished by using the SEM result shown in **Figure 4(b)** to make a map of the refractive and then numerically solving Equation (2) for the modes, realizing that the spatial inhomogeneity remains substantially axially invariant over large distances. This was done for the two cases where the elongated droplet phase was the higher index phase and then the lower index phase. From **Figure 4(a)** one observes the multiplicity of modes that can propagate. This represents a true example of Anderson localization.

5. Examples of Imaging

In the picture below in **Figure 5** is shown the image transfer property in a sample that is in a larger diameter cane form.

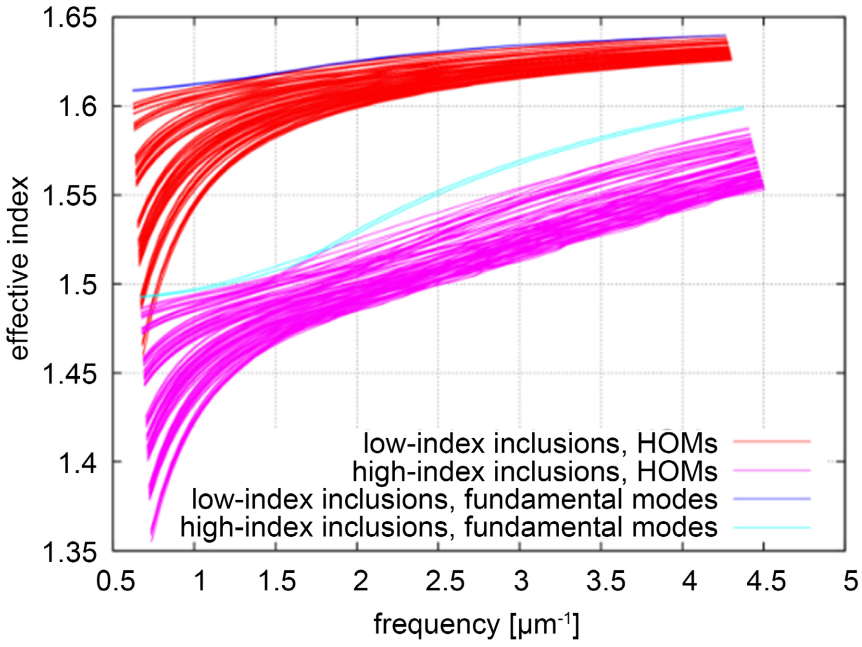

(a)

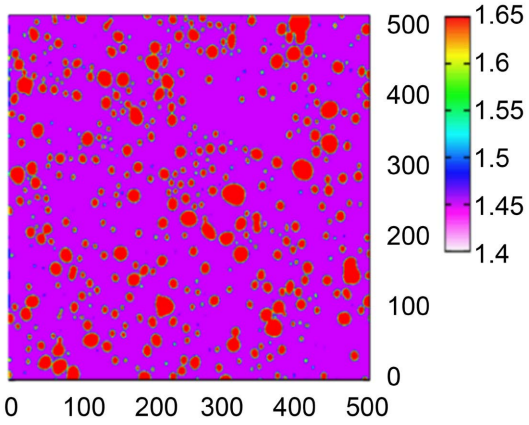

(b)

Figure 4. (a) Calculation of modes obtained from the refractive index map estimated from SEM image on RHS using numerical solution of Equation (2); (b) refractive index distribution used for the results in (a).

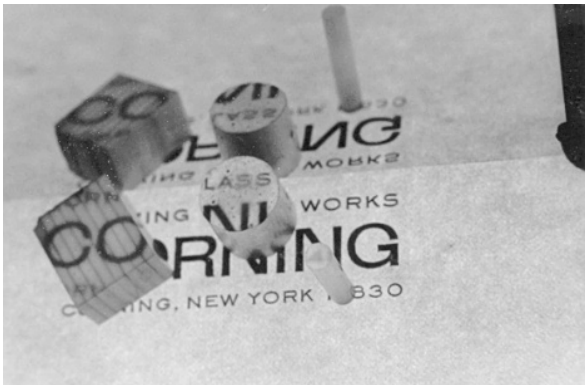

Figure 5. Example of image transfer from a much larger diameter bulk sample.

In the following two Figures, pictures are shown of images from 0.5-mm fiber samples; Figure 6 indicating the resolution and Figure 7 indicating the longest length where an image can be transmitted.

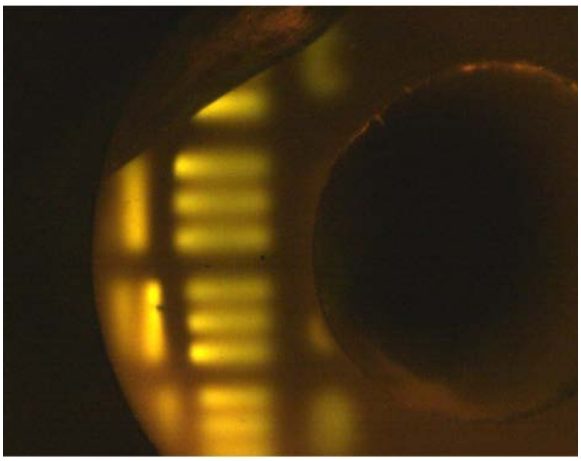

Figure 6. Image transfer from input face to exit face a 19 lp/mm resolution chart element from phase-separated borosilicate cane fiber 0.5-mm diameter 2-cm long.

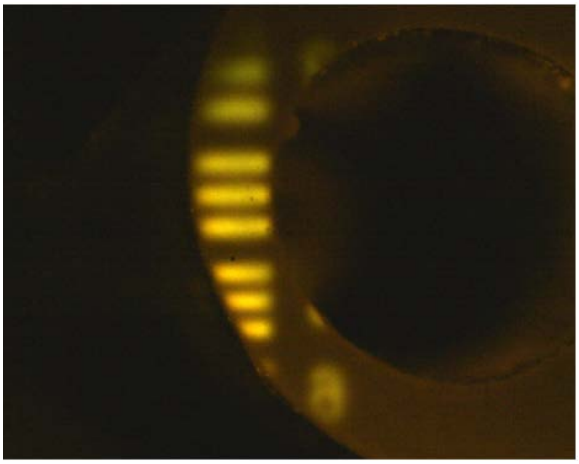

Figure 7. Image transfer of a bar pattern from a 13-cm long, 0.5-mm diameter, phase-separated Pb-borate fiber.

Compositions of the two fibers of Figure 6, Figure 7 (wt%).

compound	Figure 6	Figure 7
SiO_2	62.1	0.05
B_2O_3	13.3	69.45
PbO	0	30
Al_2O_3	2.2	0.5
Na_2O	2.7	0
P_2O_5	2.1	0
CaO	4.1	0
BaO	13.5	0

6. Conclusion

Imaging via an Anderson localization mechanism in an optical fiber can be produced from a particle-elongated, phase-separated glass medium. The approach suggests a more manufacturable approach to producing such fibers.

Acknowledgements

We wish to thank Joseph Schroeder, Derek Webb, and Heath Filkins for technical support in the processing of the glasses reported in this paper.

Conflicts of Interest

The authors declare no conflicts of interest regarding the publication of this paper.

References

[1] Anderson, P.W. (1958) *Physical Review*, **109**, 1492-1505. https://doi.org/10.1103/PhysRev.109.1492

[2] Segev, M., Silberberg, Y. and Christodoulides, D.N. (2013) *Nature Photonics*, **7**, 197-204. https://doi.org/10.1038/nphoton.2013.30

[3] Wiersma, D., Bartolini, P., Lagendijk, A., *et al.* (1997) *Nature*, **390**, 671-673. https://doi.org/10.1038/37757

[4] Karbasi, S., *et al.* (2014) *Nature Communications*, **5**, 3362. https://doi.org/10.1038/ncomms4362

[5] Randall, L.J. and Seward III, T.P. (1975) US Patent 3,870,399, "Pseudo-Fiber Optic Devices," March 11.

[6] Seward III, T.P. (1977) Proceedings of the Physics of Non-Crystalline Solids, Fourth International Conference. Transtech Publications, Aedermannsdorf, Switzerland, 342-347.